A Computationally Efficient Generalized Poisson Solution for Independent Double-Gate Transistors

Avinash Sahoo, Pankaj Kumar Thakur, and Santanu Mahapatra, *Member, IEEE*

Abstract—**Previous techniques used for solving the 1-D Poisson equation (PE) rigorously for long-channel asymmetric and independent double-gate (IDG) transistors result in potential models that involve multiple intercoupled implicit equations. As these equations need to be solved self-consistently, such potential models are clearly inefficient for compact modeling. This paper reports a different rigorous technique for solving the same PE by which one can obtain the potential profile of a generalized IDG transistor that involves a single implicit equation. The proposed Poisson solution is shown to be computationally more efficient for circuit simulation than the previous solutions.**

Index Terms—**Compact modeling, double-gate (DG) MOSFET.**

I. Introduction

THE independent double-gate (IDG) MOSFET has received considerable attention in recent years owing to its ability to modulate threshold voltage and transconductance dynamically. The modeling of the long-channel potential by solving the 1-D Poisson equation (PE) is the most fundamental step toward developing surface-potential-based core compact models for such transistors. Lu and Taur [1] have solved this PE for the asymmetric double-gate (DG) case, and their potential model involves two coupled implicit equations. Their model can be generalized for the IDG transistor by changing the boundary conditions appropriately. Nevertheless, Ortiz-Conde *et al.* [2] and Liu *et al.* [3] have proposed another solution for the potential of the IDG transistor that involves three intercoupled implicit equations. Such potential models are not efficient for compact modeling purposes as these equations need to be solved self-consistently. In this paper, we report a different technique for solving the same PE by which one can obtain a potential profile for a generalized IDG transistor that involves a single implicit equation. The proposed technique is shown to be much more computationally efficient than the others.

II. Model Development

Assuming the gradual channel approximation to be applicable for long-channel devices, the corresponding PE for the

undoped body IDG-MOSFET is given by

$$\frac{d^2\psi}{dy^2} = \frac{qn_i}{\varepsilon_{\text{Si}}} e^{\beta(\psi - V)}. \qquad (1)$$

The boundary conditions, BC1 and BC2 are, respectively, given by

$$\left. \frac{-d\psi}{dy} \right|_{y=-\frac{t_{\text{Si}}}{2}} = \frac{C_{\text{ox}1}}{\varepsilon_{\text{Si}}} (V_{\text{gs}1} - \psi_1) \qquad (2)$$

$$\left. \frac{-d\psi}{dy} \right|_{y=\frac{t_{\text{Si}}}{2}} = \frac{C_{\text{ox}2}}{\varepsilon_{\text{Si}}} (\psi_2 - V_{\text{gs}2}). \qquad (3)$$

Here, $\psi(y)$ is the electrostatic potential referenced to the Fermi potential at source, $C_{\text{ox}1(2)}$ is the capacitance per unit area of the first (second) gate, which is defined as $\varepsilon_{\text{ox}}/t_{\text{ox}1(2)}$, q is the elementary charge, ε_{Si} and ε_{ox} are the permittivities, t_{Si} and t_{ox} are the thicknesses of Silicon and SiO$_2$, respectively, β is the inverse thermal voltage, n_i is the intrinsic carrier density, and V is the electron quasi-Fermi potential. $\psi_{1(2)}$ refers to the Si/SiO$_2$ interface potential at $y = \mp t_{\text{Si}}/2$, with $y = 0$ being the center of the Si film. $V_{\text{gs}1(2)}$ represents the first (second) effective gate voltage, i.e., $V_{\text{gs}1(2)} = V_{\text{gs}1(2)\text{applied}} - \triangle\Phi_{1(2)}$, where $\triangle\Phi_{1(2)}$ is the work function difference at the respective gates. We ignore the hole concentration, and hence, the PE is valid for $\psi > 3/\beta$. By integrating the PE once using BC1 at the lower bound, we get

$$\int\limits_{\frac{d\psi}{dy}\big|_{y=-\frac{t_{\text{Si}}}{2}}}^{\frac{d\psi}{dy}} \left(\frac{d\psi}{dy}\right) d\left(\frac{d\psi}{dy}\right) = \frac{qn_i e^{-(\beta V)}}{\epsilon_{\text{Si}}} \int\limits_{\psi\left(\frac{-t_{\text{Si}}}{2}\right)}^{\psi} e^{(\beta\psi)} d\psi. \qquad (4)$$

Equation (4) results in

$$\frac{d\psi}{dy} = \pm\sqrt{Ae^{\beta\psi} + G_1} \qquad (5)$$

where $A = 2qn_i e^{(-\beta V)}/\beta\epsilon_{\text{Si}}$, and $G_1 = \{d\psi/dy|_{y=-t_{\text{Si}}/2}\}^2 - Ae^{(\beta\psi_1)}$. Now, if we use BC2 instead of BC1 at the lower bound of (4), we get another form of electric field, which is

$$\frac{d\psi}{dy} = \pm\sqrt{Ae^{\beta\psi} + G_2} \qquad (6)$$

where $G_2 = \{d\psi/dy|_{y=t_{\text{Si}}/2}\}^2 - Ae^{(\beta\psi_2)}$. It should be noted that G_1 and (G_2) may be positive or negative. Now, discarding the positive sign (reason to be discussed later) outside the

square root of (5) and integrating it once again with BC1, we get the following equations for $G_1 > 0$ and $G_1 < 0$, respectively:

$$\psi(y) = \frac{-2}{\beta} \ln \left[\sqrt{R_1} \sinh \left\{ \frac{\beta \sqrt{G_1}}{2} \left(y + \frac{t_{Si}}{2} \right) \right. \right.$$
$$\left. \left. + \sinh^{-1} \left(\frac{e^{\frac{-\beta \psi_1}{2}}}{\sqrt{R_1}} \right) \right\} \right] \quad (7)$$

$$\psi(y) = \frac{-2}{\beta} \ln \left[\sqrt{R_1^*} \sin \left\{ \frac{\beta \sqrt{G_1^*}}{2} \left(y + \frac{t_{Si}}{2} \right) \right. \right.$$
$$\left. \left. + \sin^{-1} \left(\frac{e^{\frac{-\beta \psi_1}{2}}}{\sqrt{R_1^*}} \right) \right\} \right]. \quad (8)$$

Similarly, discarding the negative sign outside the square root of (6) and integrating it once again with BC2, we get the following equations for $G_2 > 0$ and $G_2 < 0$, respectively:

$$\psi(y) = \frac{-2}{\beta} \ln \left[\sqrt{R_2} \sinh \left\{ \frac{\beta \sqrt{G_2}}{2} \left(-y + \frac{t_{Si}}{2} \right) \right. \right.$$
$$\left. \left. + \sinh^{-1} \left(\frac{e^{\frac{-\beta \psi_2}{2}}}{\sqrt{R_2}} \right) \right\} \right] \quad (9)$$

$$\psi(y) = \frac{-2}{\beta} \ln \left[\sqrt{R_2^*} \sin \left\{ \frac{\beta \sqrt{G_2^*}}{2} \left(-y + \frac{t_{Si}}{2} \right) \right. \right.$$
$$\left. \left. + \sin^{-1} \left(\frac{e^{\frac{-\beta \psi_2}{2}}}{\sqrt{R_2^*}} \right) \right\} \right]. \quad (10)$$

Here, $R_{1(2)} = A/G_{1(2)}$, $R_{1(2)}^* = -R_{1(2)}$, and $G_{1(2)}^* = -G_{1(2)}$. Therefore, the potential can take four different forms, depending on the applied bias conditions. In (7)–(10), the unknowns are the surface potentials ψ_1 and ψ_2, respectively. By applying the remaining BC2 (which was not taken during integration) to (7) and (8), we get two implicit equations as follows:

$$\sqrt{G_1} \coth(\theta_1) = \frac{C_{ox2}}{\epsilon_{Si}} \left[\frac{-2}{\beta} \ln \left\{ \sqrt{R_1} \sinh(\theta_1) \right\} - V_{gs2} \right] \quad (11)$$

$$\sqrt{G_1^*} \cot(\theta_1^*) = \frac{C_{ox2}}{\varepsilon_{Si}} \left[\frac{-2}{\beta} \ln \left\{ \sqrt{R_1^*} \sin(\theta_1^*) \right\} - V_{gs2} \right]. \quad (12)$$

Similarly, by applying BC1 to (9) and (10), we get two implicit equations in ψ_2 as follows:

$$-\sqrt{G_2} \coth(\theta_2) = \frac{C_{ox1}}{\epsilon_{Si}} \left[\frac{2}{\beta} \ln \left\{ \sqrt{R_2} \sinh(\theta_2) \right\} + V_{gs1} \right] \quad (13)$$

$$-\sqrt{G_2^*} \cot(\theta_2^*) = \frac{C_{ox1}}{\varepsilon_{Si}} \left[\frac{2}{\beta} \ln \left\{ \sqrt{R_2^*} \sin(\theta_2^*) \right\} + V_{gs1} \right]. \quad (14)$$

Here, $\theta_{1(2)} = \beta(\sqrt{G_{1(2)}} t_{Si}/2) + \sinh^{-1}\{e^{-\beta \psi_{1(2)}/2}/\sqrt{R_{1(2)}}\}$, and $\theta_{1(2)}^* = \beta(\sqrt{G_{1(2)}^*} t_{Si}/2) + \sin^{-1}\{e^{-\beta \psi_{1(2)}/2}/\sqrt{R_{1(2)}^*}\}$. It is worth noting that in the previous works [1]–[3], the potential models involve multiple intercoupled implicit equations. For the asymmetric DG case, the roots of these equations may be precalculated and stored in a lookup table [1]. However, for the IDG transistor, these roots have to be calculated during circuit simulation [3]. It is also found that these equations sometimes have very closely located multiple roots, and it is extremely tedious to choose the correct set. Therefore, the practical application of previous potential models in a circuit simulator is questionable. It is worth noting that the solution techniques reported in previous works do not take any of the boundary conditions while deriving the general form. In this paper, we take one boundary condition into account while deriving the general solution from the main PE. As a result, the general form of the solutions obtained in previous works needs to be subjected to two boundary conditions that lead to two or three implicit equations (depending on minor differences in the approaches to their works). On the contrary, we need to apply our four different forms of "general solution" to the one remaining boundary condition. As a result, the proposed model involves only one implicit equation per form, i.e., one out of the four equations (11)–(14). The roots of these implicit equations (ψ_1 or ψ_2) are always found to be nearest to the G-zero-point (GZP) ($\psi_{1(2)} @ G_{1(2)} = 0$). We shall now explain the reason behind discarding one of the signs outside the square root in (5) and (6). It should first be noted that $d^2\psi/dy^2$ is always positive, and hence, $\psi(y)$ cannot have a maxima inside the domain. Since $d\psi/dy$ is a monotonically increasing function, $\psi(y)$ can have only one minima. If we also consider the fact that the sign of the electric field does not change at the Si/SiO_2 interface, we can say that if $V_{gs1} > V_{gs2}$, then $d\psi/dy$ has to be negative, at least in the small neighborhood of $y = -t_{Si}/2$. Similarly, when $V_{gs1} < V_{gs2}$, $d\psi/dy$ has to be positive, at least in the small neighborhood of $y = t_{Si}/2$. As we have used BC1 in (5), we should discard the positive $d\psi/dy$ since we can only ensure a negative $d\psi/dy$ in the neighborhood of $y = -t_{Si}/2$ when $V_{gs1} > V_{gs2}$. Similarly, we discarded the negative $d\psi/dy$ in (6) as we here used BC2, and $d\psi/dy$ has to be positive in the neighborhood of $y = t_{Si}/2$ when $V_{gs1} < V_{gs2}$. Now, $d\psi/dy$ calculated from (7) or (9) has a *coth* function. Thus, $\psi(y)$ cannot have a minima inside the domain even, when $G_{1(2)} \to 0$. Therefore, (7) and (9) model a case when $\psi(y)$ is strictly monotonic inside the film. However, $\psi(y)$ obtained from (8) or (10) may have a minima inside the domain as $d\psi/dy$ has a *cot* function. Therefore, though we discarded the positive (negative) sign of $d\psi/dy$ in (5) and (6), both (8) and (10) can handle those cases where the minima of $\psi(y)$ exists. Thus, the cardinal point is that both the sign of the root and the sign of $G_{1(2)}$ determine the nature of the potential profile. Since (7)–(10) take care of minima and no-minima cases, they can predict any combination of bias in the IDG-MOSFET. Note that for $V_{gs1} = V_{gs2}$, one can use either (8) or (10).

Now, we discuss the procedure of choosing *one out of the four* forms of $\psi(y)$ based on the bias conditions. The discussion above makes it clear that when $V_{gs1} \geq V_{gs2}$, one has to choose

(7) or (8) or, otherwise, choose (9) or (10). In the next step, one has to use the concept of the GZP and critical voltage to select the exact form from the chosen set as discussed in the next paragraph. Finally, one should solve the corresponding implicit equation (11)–(14), i.e., *only one* implicit equation at any given bias, for the calculation of the potential profile. As (7) and (8) [and similarly (9) and (10)] were derived on the basis of the sign of G, the GZP plays a major role in determining the final form of the solution. The GZP is that interface potential at which G becomes zero. Hence, we can have two GZPs, depending on which G we choose in the first step. For example, if one chooses (7) or (8) in the first step, then one should use the GZP corresponding to G_1 denoted by ψ_{gzp1}; otherwise, one should use ψ_{gzp2}. Equating $G_{1(2)}$ to zero and solving for the interface potential $\psi_{1(2)}$, we get the explicit formulation for the GZP as follows:

$$\psi_{\text{gzp1(2)}} = V_{\text{gs1(2)}} - \frac{2}{\beta} W \left\{ \frac{\beta}{2} e^{\left(\frac{\beta V_{\text{gs1(2)}}}{2} \right)} \sqrt{\frac{A \varepsilon_{\text{Si}}^2}{C_{\text{ox1(2)}}^2}} \right\}. \quad (15)$$

Here, W represents the Lambert function. Interestingly, $\psi_{\text{gzp1(2)}}$ is approximately equal to the surface potential of an undoped bulk MOSFET as proposed by Shangguan *et al.* [5].

In Fig. 1(a), G_1 is plotted as a function of the interface potential ψ_1 for two different values of V_{gs1}. The circles represent the values of ψ_1 obtained from (11) or (12) for different V_{gs2}'s ($\leq V_{\text{gs1}}$), and they increase with increasing V_{gs2}. To choose the correct form between (7) and (8), one has to determine whether the correct ψ_1 for the given bias lies to the left or the right side of ψ_{gzp1}, i.e., whether it lies in the positive or negative G_1 region. ψ_1 shifts toward the negative G_1 region [where (8) holds] when one increases V_{gs2} because the opposing electric field from the second gate increases the possibility of having a minima of $\psi(y)$ inside the Si film. Thus, we introduce a term called critical voltage (V_{gscrit}), which is that V_{gs2} at which ψ_1 obtained from (11) or (12) becomes equal to ψ_{gzp1}. One can derive the expression for the V_{gs2crit} by applying the limit $G_1 \to 0$ to (11) and (12) and then replacing ψ_1 by ψ_{gzp1} and V_{gs2} by V_{gs2crit}. Similarly, V_{gs1crit} can be derived by applying the limit $G_2 \to 0$ to (13) and (14) and then replacing ψ_2 by ψ_{gzp2} and V_{gs1} by V_{gs1crit} as follows:

$$V_{\text{gs2(1)crit}} = \left[\frac{-2}{\beta} \ln \left\{ \frac{\beta \sqrt{A} t_{\text{Si}}}{2} + e^{\frac{-\beta \psi_{\text{gzp1(2)}}}{2}} \right\} \right.$$
$$\left. - \frac{\varepsilon_{\text{Si}} \sqrt{A}}{C_{\text{ox2(1)}} \left[\frac{\beta \sqrt{A} t_{\text{Si}}}{2} + e^{\frac{-\beta \psi_{\text{gzp1(2)}}}{2}} \right]} \right]. \quad (16)$$

Therefore, for $V_{\text{gs2(1)}} > V_{\text{gs2(1)crit}}$, one has to choose the $G_{1(2)} < 0$ form, i.e., (8) or (10), otherwise, one has to choose between (7) and (9). In Fig. 1(b), we have shown the variation of ψ_{gzp} and V_{gscrit} as a function of the quasi-Fermi level (V), and both of these quantities are found to be saturated at a high V as they depend on the square root of A.

Now, coming to the question of the continuity of the proposed model between various forms, we notice that when
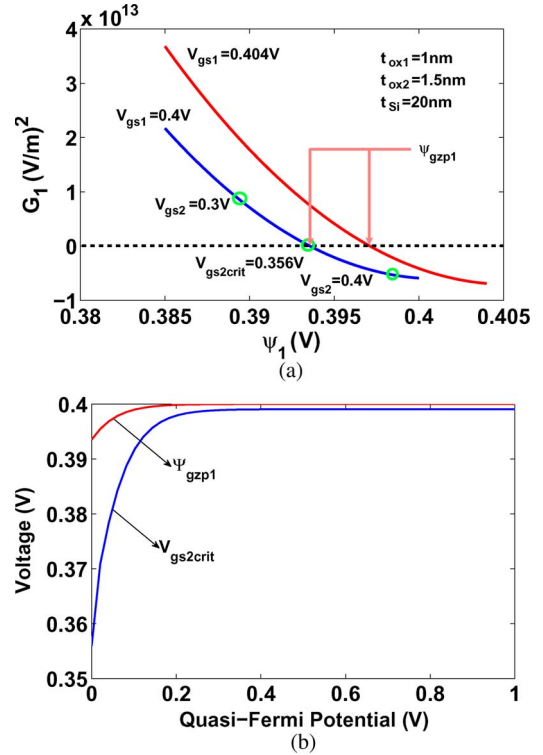

Fig. 1. (a) GZP and critical voltage at $V = 0$. (b) Variation of ψ_{gzp1} and V_{gs2crit}, with quasi-Fermi level V for the same parameters at $V_{\text{gs21}} = 0.4$ V.

$G_{1(2)} \to 0$, (7)–(10) merge to the following limit values:

$$\lim_{G_1 \to 0} \psi(y) = \frac{-2}{\beta} \ln \left\{ e^{\frac{-\beta \psi_1}{2}} + \frac{\beta \sqrt{A}}{2} \left(y + \frac{t_{\text{Si}}}{2} \right) \right\} \quad (17)$$

$$\lim_{G_2 \to 0} \psi(y) = \frac{-2}{\beta} \ln \left\{ e^{\frac{-\beta \psi_2}{2}} + \frac{\beta \sqrt{A}}{2} \left(-y + \frac{t_{\text{Si}}}{2} \right) \right\}. \quad (18)$$

Equations (17) and (18) prove the continuity of the model between (7)–(10), respectively. Again, when $d\psi/dy \to 0$, ψ becomes ψ_1 as per (7) and (8). Similarly, ψ becomes ψ_2 as per (9) and (10) when $d\psi/dy \to 0$, but $\psi_2 = \psi_1$ at $d\psi/dy = 0$. Therefore, the proposed model is also continuous between the G_1 and G_2 forms. It is worth noting that the previous works [1]–[3] use two different forms (hyperbolic and trigonometric) to model $\psi(y)$. A similar critical voltage concept has been used in the models [1], [3] to choose between the two forms. However, the formulation for critical voltage is implicit in their work, whereas it is explicit in this work. There are some similarities between the solution techniques used in this work and the work reported in [5]. However, the previous work uses only *trigonometric* forms and, thus, is not valid under all bias conditions. The same group has also proposed a surface potential equation (not the full Poisson solution) that uses a single implicit equation [6]. As in their other work, it is also based on *trigonometric* forms and is not valid under all bias conditions.

III. RESULTS AND DISCUSSIONS

In Figs. 2 and 3, we validated our model against a numerical simulation for $V = 0$. The numerical solution of the PE is
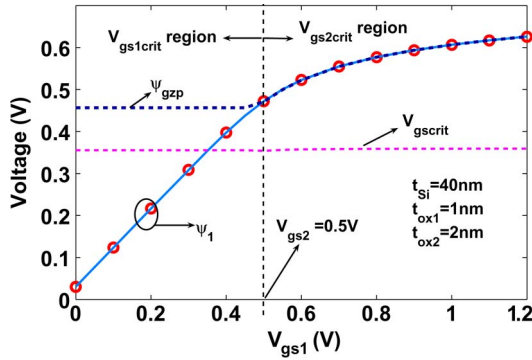
Fig. 2. Validation of the continuity of the proposed model over the gate voltage variation. Here, the line represents the model, and the symbol represents numerical simulations. To the left side of the $V_{gs2} = 0.5$ V line, $V_{gs1} < V_{gs2}$, and hence, $\psi_{gzp} = \psi_{gzp2}$. To the right side of the $V_{gs2} = 0.5$ V line, $V_{gs1} > V_{gs2}$, and hence, $\psi_{gzp} = \psi_{gzp1}$. Similarly, V_{gscrit} is $V_{gs1crit}$ to the left of the dotted line, and V_{gscrit} is $V_{gs2crit}$ to the right side of the dotted line.
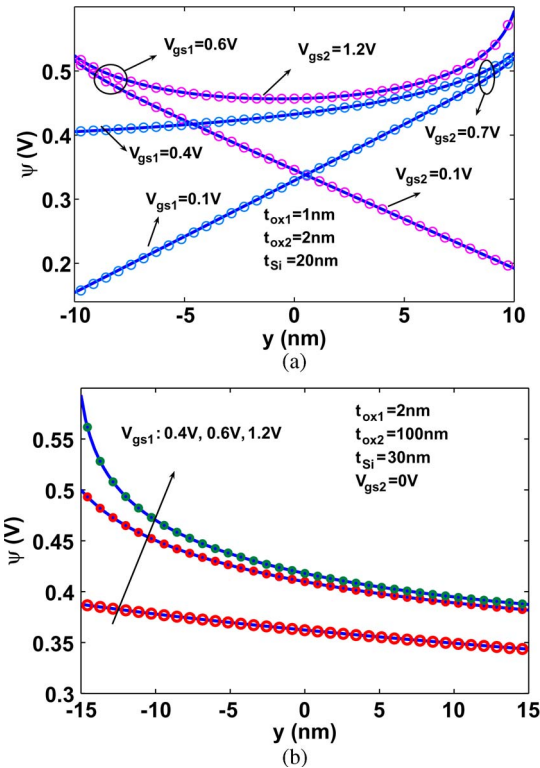

(a)

(b)

Fig. 3. Potential profile for (a) IDG-MOSFET and (b) single-gate SOI MOSFET for different bias conditions. Here, the line represents the proposed model, and the symbol represents the numerical simulation.

obtained using the COMSOL Multiphysics software [6]. Fig. 2 also shows the variation of the GZP and critical voltages under different bias conditions. Though different numerical recipes are available to solve a system of nonlinear equations, in order to obtain a fair comparison between different models, we have implemented them in MATLAB [8]. The "trust region technique" [9] is used to find the roots of the implicit equations. For a particular device, we solve those equations for a wide range of gate voltages to ensure both trigonometric and hyperbolic operation. It is found that the time taken to solve coupled implicit equations [1], [3] are, on the average, *five* times higher than that taken for a single implicit equation as shown in Fig. 4. This is to be expected as a system of multidimensional
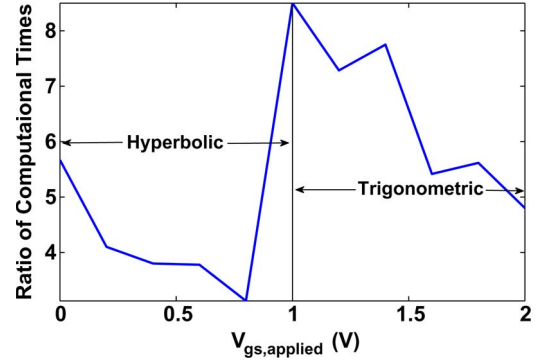

Fig. 4. Ratio of the computational times between the previous model [1] and the proposed model for an asymmetric DG transistor with the following device parameters: $t_{ox1} = 1.5$ nm; $t_{ox2} = 1.5$ nm; $t_{si} = 10$ nm; $\Delta\Phi_1 = -0.56$ V; and $\Delta\Phi_2 = 0.56$ V. The characteristic is almost independent of the values of V.

nonlinear equations is much more difficult to solve than a 1-D system [10]. In our model, the initial guess is always fixed very close to ψ_{gzp} (on the order of $\pm 10^{-6}$ V, depending on the sign of G). As a proper initial guess is not available in [1] and [3], we have solved those equations using different initial guesses and have taken the best value. This is also another reason for the proposed Poisson solution technique being faster than the others. Therefore, the GZP point serves the following two purposes: 1) to guide the user to choose one out of the four forms of the potential model and 2) to provide initial guesses for the surface potential calculation. The difference between the initial guess and the root is found to vary between 10^{-3} and 10^{-6} V, depending on the applied bias. It is worth noting that as the proposed Poisson solution involves a single implicit equation, it might be possible to calculate the surface potential explicitly after following the recipes given in [11]. Finally, it should be mentioned that the complexity of the ψ_{gzp} equation, which involves Lambert's function, is in the same order of the equation involving the "s" parameter in [1] and [3]. However, Lambert's function is a very well-studied function and is also available in the GNU scientific library [12]. We can therefore expect that the computational efficiency of ψ_{gzp} would be free from initial guesses, which is not the case for the "s" parameter.

IV. CONCLUSION

The 1-D PE for the long-channel IDG MOSFET has been rigorously solved in order to obtain the potential profile. Unlike the previous work, where the potential model depends on the self-consistent solution of multiple implicit equations, the proposed solution technique involves only a single implicit equation. The proposed Poisson solution is shown to be continuous over all bias conditions and therefore appears to be more efficient for compact modeling purposes.

ACKNOWLEDGMENT

REFERENCES

[1] H. Lu and Y. Taur, "An analytic potential model for symmetric and asymmetric DG MOSFETs," *IEEE Trans. Electron Devices*, vol. 53, no. 5, pp. 1161–1168, May 2006.

[2] A. Ortiz-Conde, F. J. García-Sánchez, J. Muci, S. Malobabic, and J. J. Liou, "A review of core compact models for undoped double gate SOI MOSFETs," *IEEE Trans. Electron Devices*, vol. 54, no. 1, pp. 131–140, Jan. 2007.

[3] F. Liu, J. He, Y. Fu, J. Hu, W. Bian, Y. Song, X. Zhang, and M. Chan, "Generic carrier-based core model for undoped four-terminal double-gate MOSFETs valid for symmetric, asymmetric, and independent-gate-operation modes," *IEEE Trans. Electron Devices*, vol. 55, no. 3, pp. 816–826, Mar. 2008.

[4] A. Ortiz-Conde, F. J. García Sánchez, and M. Guzman, "Exact analytical solution of channel surface potential as an explicit function of gate voltage in undoped-body MOSFETs using the Lambert W function and a threshold voltage definition there from," *Solid State Electron.*, vol. 47, no. 11, pp. 2067–2074, Nov. 2003.

[5] W. Z. Shangguan, T. C. Au Yeung, Z. M. Zhu, and X. Zhou, "General analytical Poisson solution for undoped generic two-gated metal–oxide–semiconductor field-effect transistors," *Appl. Phys. Lett.*, vol. 90, no. 1, p. 012 110, Jan. 2007.

[6] Z. Zhu, X. Zhou, K. Chandrasekaran, S. C. Rustagi, and G. H. See, "Explicit compact surface-potential and drain-current models for generic asymmetric double gate metal–oxide–semiconductor field-effect-transistors," *Jpn. J. Appl. Phys.*, vol. 46, no. 4B, pp. 2067–2072, Apr. 2007.

[7] Users' Manual of Comsol Multiphysics, COMSOL AB, Stockholm, Sweden, 2009. [Online]. Available: www.comsol.com

[8] Users' Manual of MATLAB, The MathWorks, Inc., MA, USA, 2009. [Online]. Available: www.mathworks.com

[9] T. F. Coleman and Y. Li, "An interior, trust region approach for non-linear minimization subject to bounds," *SIAM J. Optim.*, vol. 6, no. 2, pp. 418–445, May 1996.

[10] W. H. Press, B. P. Flannery, and W. T. Vetterling, *Numerical Recipes in C: The Art of Scientific Computing*. Cambridge, U.K.: Cambridge Univ. Press, 1992.

[11] B. Yu, H. Lu, M. Liu, and Y. Taur, "Explicit continuous models for double-gate and surrounding-gate MOSFETs," *IEEE Trans. Electron Devices*, vol. 54, no. 10, pp. 2715–2722, Oct. 2007.

[12] Users' Manual of GNU Scientific Library, Free Software Foundation, Inc., Boston, MA 02110-1301, USA, 2009. [Online]. Available: http://www.gnu.org/software/gsl/

Pankaj Kumar Thakur received the B.Eng. degree in electrical and electronics engineering from Sri Chandrasekharendra Saraswathi Viswa Mahavidyalaya (Deemed University), Kanchipuram, India, in 2006 and the M.Eng. degree in Microelectronics from the Birla Institute of Technology and Science, Pilani, India, in 2008.

He is currently pursuing his PhD at Nano Scale Device Research Laboratory, Centre for Electronics Design and Technology, Indian Institute of Science, Bangalore, India. His research interests include the physics and modeling of semiconductor devices and designing analog mixed-signal RF circuits using advanced- and post-CMOS devices.

Santanu Mahapatra (M'08) received the B.E. degree in electronics and telecommunication from Jadavpur University, Kolkata, India, in 1999, the M.Tech. degree in electrical engineering, with specialization in microelectronics, from the Indian Institute of Technology, Kanpur, India, in 2001, and the Ph.D. degree in electrical engineering, from the Swiss Federal Institute of Technology Lausanne (EPFL), Lausanne, Switzerland, in 2005. In his Ph.D., he worked on compact modeling of single electron transistors and their hybridization with CMOS.

Since 2005, he has been an Assistant Professor at the Centre for Electronics Design and Technology (CEDT), Indian Institute of Science, Bangalore, India. He founded the Nano Scale Device Research Laboratory at the CEDT in 2006, where his team is engaged in research on compact modeling and simulation of emerging nanotechnologies and advanced CMOS devices. He has supervised several doctoral dissertations and masteral theses. He is the author and coauthor of several papers published in international journals and refereed conference proceedings. He is also the author of the book *Hybrid CMOS Single Electron Transistor Device and Circuit Design* (Artech House, 2006). His current research interests include device reliability, multigate transistors, tunnel field-effect transistors, single-electron transistors, and CMOS nanohybridization.

Dr. Mahapatra received the Best Paper Award in the International Semiconductor Conference (CAS), Romania, in 2003. He also received the IBM Faculty Award in 2007, the Microsoft India Research Outstanding Faculty Award in 2007, and the associateship in the Indian Academy of Science in 2009.

Avinash Sahoo received the B.Tech degree in electronics and telecommunications from the Institute of Technical Education and Research, Bhubaneswar, India, in 2007, and the M.Sc.(Eng.) degree in electronics design from the Indian Institute of Science, Bangalore, India, in 2009.

He is currently with the Nano Scale Device Research Laboratory, Centre for Electronics Design and Technology, Indian Institute of Science, Bangalore. His research interests include the modeling and simulation of nanoscale semiconductor devices.